Available online at www.CivileJournal.org

Civil Engineering Journal

(E-ISSN: 2476-3055; ISSN: 2676-6957)

Vol. 12, No. 01, January, 2026

Seepage Control in Zoned Earth Dams Using Lime–Fly Ash Treated Sandy Soil

Ali M. Madhloom [1*], Abdulaziz A. Al-Kifae [1], Saleh I. Khassaf [2]

[1] *Department of Civil Engineering, College of Engineering, Al-Nahrain University, Baghdad, Iraq.*

[2] *Department of Civil Engineering, College of Engineering, University of Basrah, Basrah, Iraq.*

Received 21 October 2025; Revised 11 December 2025; Accepted 16 December 2025; Published 01 January 2026

Abstract

Seepage control is a critical factor in ensuring the stability of earth dams, particularly those constructed with permeable soils. Uncontrolled seepage and increased pore pressures within the dam body are typically associated with instability, internal erosion, and potential failure. This study aims to evaluate the effectiveness of lime–fly ash mixtures in controlling seepage through earth dams constructed with sandy soil, using experimental modelling and numerical simulation. A physical model of a zoned earth dam was built using untreated sandy soil as the control model, along with treated models in which the sandy core was stabilized with progressively higher lime–fly ash proportions. The results of laboratory permeability tests demonstrated significant reductions in hydraulic conductivity with increasing additive content, resulting in delayed steady-state conditions and a reduction of up to 98.2% in seepage rate compared with the control model. Numerical simulations, validated against experimental results (coefficient of determination, R^2>0.98), accurately reproduced phreatic lines and seepage rates and were further used to examine the influence of core slope geometry. The results showed that a core slope of 0.75:1 provided nearly equivalent hydraulic performance to that of the baseline 1:1 slope, offering a more cost-effective alternative. These findings highlight the potential of lime–fly ash–sand mixtures as sustainable and cost-efficient alternatives for dam cores, particularly in regions where clay resources are limited.

Keywords: Permeability; Lime-Fly Ash Additives; Seepage; Sandy Soil; Earth Dam.

1. Introduction

Earth dams are critical infrastructures worldwide, serving functions such as water storage, flood control, and irrigation. A major challenge to their stability and performance is seepage through the dam body or foundation, which, if uncontrolled, can lead to internal erosion, piping, and potentially catastrophic failure [1]. Effective design must therefore focus on controlling both the magnitude and distribution of seepage [2]. Flow through earth dams is an important design consideration. It must be ensured that the pore-water pressure at the downstream end does not cause instability, and that the exit hydraulic gradient does not cause piping [3]. Several experimental and numerical studies have been conducted to assess the seepage rates [4, 5] and to explore methods for reducing them [6-8]. Taghvaei et al. [9] investigated the impact of powdery nano-clay on the seepage rate**.** The experiments were conducted by constructing an impermeable blanket on the reservoir side of the earth dam using a mixture of sandy soil and varying amounts of montmorillonite nano-clay. The results indicated that increasing the nano-clay content reduced seepage rate. Alzamily & Abed [10] evaluated the permeability of sandy soils enhanced with additives as an alternative core material for earth dams. The study showed that sand mixed with 10% cement kiln dust and 5% cement achieved a 99.6% reduction in

* Corresponding author: ali.muzher@buog.edu.iq

https://doi.org/10.28991/CEJ-2026-012-01-04

permeability. Haman et al. [11] suggested various dam sealing methods, including blankets, bentonite, and chemical additives, emphasizing that the appropriate method depends on whether the soil is coarse-grained or fine-grained. Shuhaib & Khassaf [12] investigated the use of tire rubber powder (TRP) as an additive to enhance earth-dam cores and reduce seepage. The findings showed reductions in seepage rate, with the 50% TRP mixture achieving up to a 41.5% decrease in seepage, while lower ratios showed noticeably weaker performance. Onyelowe et al. [13] studied the use of a double-textured High-Density Polyethylene (HDPE) geomembrane barrier in embankments. Two improvement techniques were evaluated: covering the upstream slope with an HDPE geomembrane stabilized with gabions, and combining this geomembrane with a downstream rock toe. The study demonstrated that these measures can effectively enhance both seepage control and slope stability.

To reduce soil permeability, lime and fly ash additives have recently been adopted as an effective method. The pozzolanic properties of fly ash allow it to react with hydrated lime to create cementitious materials [14]. Several studies have reported optimal proportions of lime and fly ash for soil stabilization. Effective mixtures can be prepared using 10–35% fly ash with 2–10% lime [14]. Ratios of 1:3 and 1:4 (lime to fly ash) are most common for economic and performance purposes, generally corresponding to 10–15% fly ash and 2.5–4% lime [15]. Sandy soils typically show poor response to lime alone but can be stabilized with pozzolanic additives such as fly ash or clay, with recommended ranges of 10–20% fly ash and 3–5% lime [16]. In general, recommended proportions for soil stabilization fall between 10% and 20% fly ash and 3% and 7% lime [17]. Several studies have utilized lime and fly ash to enhance the geotechnical and hydraulic properties of soil [18-21]. Di Sante et al. [22] examined the permeability and shear behavior of low-plasticity clay treated with fly ash alone and with a fly ash–quicklime blend. The results showed that the combined treatment initially increased hydraulic conductivity at optimum water content, followed by a limited reduction during curing as pozzolanic gels formed, while also improving shear strength and reducing compressibility.

Sharif et al. [23] investigated the geotechnical and economic effects of stabilizing clayey subgrade soil with lime and fly ash for pavement construction. The experiments employed an optimal mixture of 4% lime and 20% fly ash, which improved shear strength by 34%. Bhoi et al. [24] studied the stabilization of black cotton soil using varying proportions of lime and fly ash. Laboratory experiments indicated that the combined addition of 5% lime and 10% fly ash significantly improved soil strength, reduced plasticity, and increased bearing capacity. Swamynaidu & Tyagi [25] investigated the hydraulic conductivity of fly ash–cement–alkali activated (FCAA) clay mixes for use as low-permeability hydraulic barriers. The results indicated that FCAA-treated clays exhibited lower or comparable hydraulic conductivity compared to untreated clay. Husein & Chemeda [26] used lime additives to modify some of the unwanted properties of clayey soil, which is utilized to build the core of zoned earth dams, where, with the addition of 6% lime, the soil permeability decreased significantly, from 4.47×10^{-6} to 3.63×10^{-7} m/s. Garzón et al. [27] studied the improvement of engineering properties in Spanish phyllite clay with the addition of 3, 5, and 7 wt.% lime, and found that the clay–lime mixtures exhibited good compaction along with very low to extremely low permeability coefficients. According to Islam et al. [28], fly ash demonstrates greater effectiveness than lime in reducing the permeability of clayey and sandy soils in the 5–30% range.

Although previous studies have investigated the use of different additives to reduce seepage in earth dams and enhance the geotechnical properties of soils, most of these approaches depend on expensive materials, complex application methods, or are limited to using either lime or fly ash in fine-grained soils. Sandy soils, which are commonly available in many regions, generally exhibit poor performance when stabilized with lime alone. The combined use of lime and fly ash for sandy dam cores has not been studied. The novelty of this research lies in demonstrating that a properly proportioned lime–fly ash mixture can transform sandy soil into an effective alternative to clay cores, while also providing design optimization insights through numerical modeling. The importance of this study lies in its practical solution for regions where clay is scarce, thereby enhancing the safety, sustainability, and cost-effectiveness of earth dam construction.

In the present study, to minimize seepage through the body of the earth dam, the core soil of the dam was developed using sandy soil mixed with lime and fly ash additives to achieve permeability properties comparable to those of clay, which is typically used in dam cores. A numerical model of the dam was simulated in SLIDE 6.0 software to analyze the effect of core slope on pressure distribution and seepage rate. The numerical investigation further aims to determine whether reducing the core slope—and consequently the volume of impermeable material—could provide equivalent hydraulic performance while simultaneously reducing construction costs.

2. Materials and Methods

2.1. Experimental Model Design

A rectangular basin containing a model of an earth dam was designed as the experimental model (Figure 1). The unit is intended to facilitate the investigation and testing of phenomena related to the effects of water seepage through permeable media. It also examines how the seepage rate and the location of the phreatic line vary when an earth dam is improved with varying additive percentages.

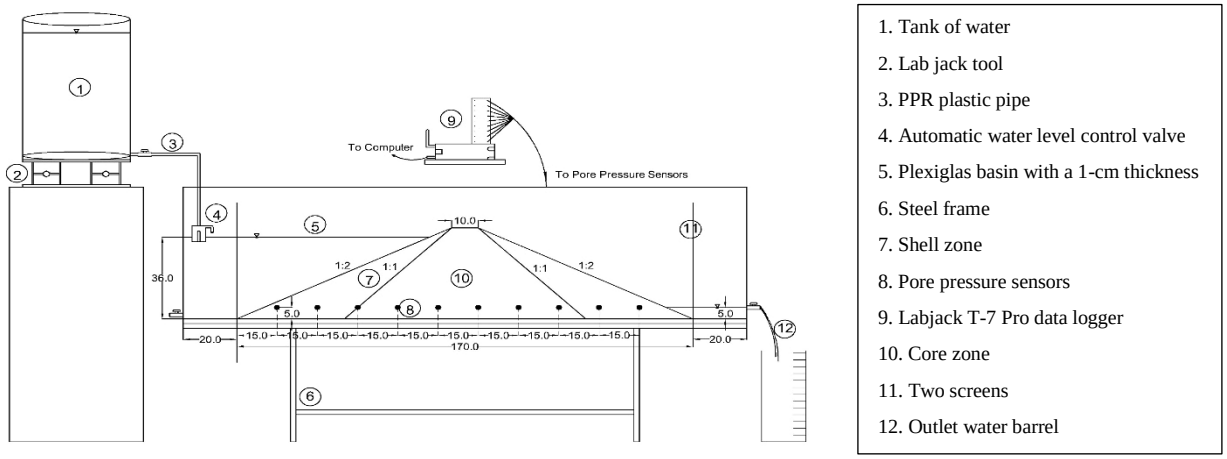

Figure 1. Experimental model layout of the earth dam (all dimensions in cm)

The cross-sectional dimensions of the physical model were not selected arbitrarily; all design criteria were carefully considered when determining the final size. The freeboard was chosen within the U.S.B.R. recommended, and the top width was calculated using the suggested formula:

$$B_t = \frac{5}{3} \cdot \sqrt{(H)} \quad (1)$$

where, H is the height of the dam.

Furthermore, the upstream and downstream slopes were specified in accordance with the soil characteristics and the type of earth dam being modeled [29, 30]. Following that, the dam geometry was scaled down to produce a model suitable for the basin. This scaling ensured practical model dimensions, allowing controlled seepage monitoring within the laboratory facility.

The earth dam was constructed at the center of the basin. The earth dam model measured 170 cm in length, 18 cm in width, and 40 cm in height. The slopes of the earth dam, both upstream and downstream, were 2:1 (horizontal: vertical) based on the soil characteristics. The maximum water level was 36 cm, and this level was maintained in all cases of the present study. The basin's internal dimensions were 210 cm (length) × 50 cm (height) × 18 cm (width), and it was built from a 1-cm-thick, collarless Plexiglas wall.

As seen in Figure 2, the lab basin was positioned 50 cm above the ground on a steel structure and leveled in all directions. The model was reinforced with thin rubber strips at the bed of the basin to guard against plexiglass breakage and to damp vibration caused by soil compaction. A water-seal glue was used to seal the seams. A laser cutter was employed to create openings for the pressure sensors, positioned 5 cm above the base of the Plexiglas basin and at horizontal distances of 0.15, 0.30, 0.45, 0.60, 0.75, 0.90, 1.05, 1.20, 1.35, and 1.50 m from the upstream toe. A raised water tank was positioned on the upstream side of the basin. The tank, with a capacity of 81.5 liters, supplied water to fill the earth-dam reservoir. A plastic pipe with an automatic float valve was used to link the tank to the basin. The function of the automatic float valve is to maintain a constant water level in the reservoir, which remains unchanged over time. It operates so that when the water level rises to the water limit line, the valve immediately stops supplying water. When the reservoir's water level falls, the valve automatically begins supplying water. The jack located below the tank controls the rise and fall of the automatic float valve level. Variations in seepage rate can be monitored by drilling a hole in the lower portion of the earth dam and connecting it to the graded water barrel on the model's right side.

The dam model was split into eight layers (each 5 cm thick after compression). To determine the required quantity of soil for each layer, the dry density of the soil at 90% compaction was calculated using the maximum dry density of the soil and the geometry of the earth dam. To compact the soil, a square standard hammer was used. The appropriate density was achieved in each layer based on the optimal water content. Pressure sensors recorded readings every 5 seconds to determine the final location of the phreatic surface. The bed of the basin functions as an impervious layer in the physical model; therefore, all seepage originates from the dam's main body. To determine the seepage rate, the outflow water from the downstream graded barrel was measured every 15 minutes. Pressure sensor readings continued in an unsteady state until a steady state was established. To calculate the location of the phreatic line in the earth dam model, 10 pressure sensors were installed and connected to the data logger.

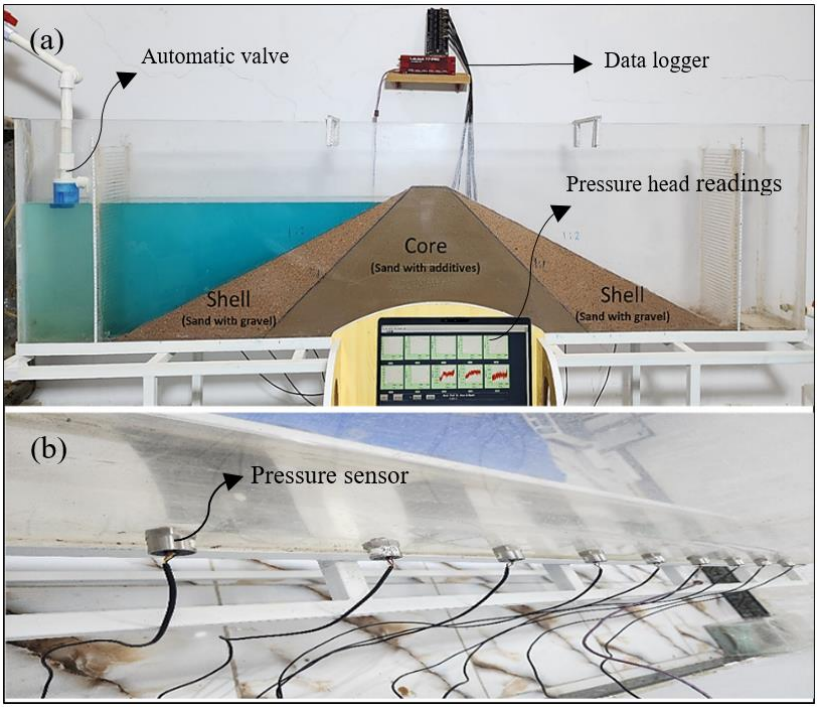

Figure 2. (a) Plexiglas basin and an earth dam model, (b) Pressure sensors

2.2. Soil of the Dam Body

Experimental studies were conducted on two locally available soils. The first type of soil represented sand with gravel, which simulated the soil found in the earth dam's shell. The second type, sandy soil, was improved using different additives to simulate the soil found in the earth dam core. Figure 3 displays the sandy soil grading curve that was used in the core zone. Since 5.2% of the particles in this sandy soil pass through a sieve with mesh No. 200, the gradation indicates that it is type A-3 (fine sand) in the AASHTO classification and Type SP (poorly graded sand) in the Unified Soil Classification System (USCS).

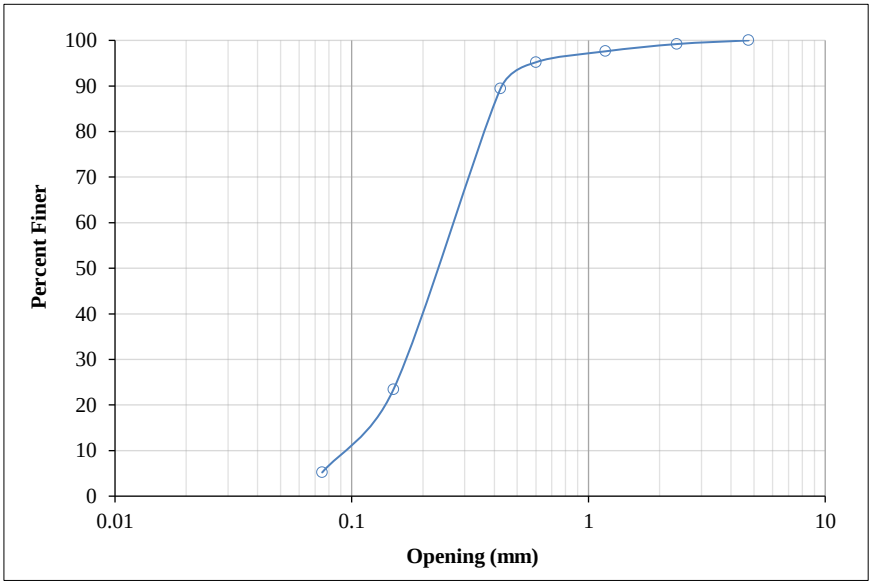

Figure 3. Grain size distribution curve of sandy soil

2.3. Lime and Fly Ash Additives

Lime and fly ash are two types of additives used to enhance the soil properties used to construct the core of the earth dam. In this investigation, hydrated lime was obtained from the Karbala Lime Factory, which manufactures it in compliance with Iraqi Standard [31]. The chemical composition of the lime used is presented in Table 1. According to the chemical analysis of fly ash obtained from laboratory testing, which is displayed in Table 2, the fly ash's chemical composition conforms to ASTM C-618 [32] requirements.

Table 1. Chemical analysis of hydrated lime

Composition	%
Silica (SiO_2)	3.26
Alumina (Al_2O_3)	0.67
Ferric oxide (Fe_2O_3)	0.22
Magnesium oxide (MgO)	0.30
Calcium oxide (CaO)	69.72
Sulfur trioxide (SO_3)	0.28
Sodium oxide (Na_2O)	0.15
L.O.I.	25.60

Table 2. Chemical analysis of fly ash measured by XRF

Composition	%
Silica (SiO_2)	58.34
Alumina (Al_2O_3)	26.62
Ferric oxide (Fe_2O_3)	3.19
Magnesium oxide (MgO)	2.88
Calcium oxide (CaO)	2.44
Sulfur trioxide (SO_3)	0.15
Sodium oxide (Na_2O)	0.65
L.O.I.	2.80

2.4. Soil Mixing with Additives

In the core zone, sandy soil was combined with four percentages of lime-fly ash additives. These percentages, measured by weight of dry soil in the core, were: 3% Lime + 9% Fly ash, 5% Lime + 15% Fly ash, 7% Lime + 21% Fly ash, and 9% Lime + 27% Fly ash. As a result, many models were developed for the research, and these models were assigned codes, which are displayed in Table 3. These values were chosen in accordance with proportions recommended in the literature.

Table 3. Codes of the different models being studied

Lime + Fly ash (% by weight)	Model code
0	Control model
3% Lime + 9% Fly ash	M-1
5% Lime + 15% Fly ash	M-2
7% Lime + 21% Fly ash	M-3
9% Lime + 27% Fly ash	M-4

The permeability of soil samples was determined using two standard laboratory tests, the constant head test and the falling head test, as specified in ASTM D-2434 [33] and ASTM D-5084 standards [34]. The samples in each test were compacted to 90% of their maximum density in layers at the optimum moisture content. When calculating the sample weight of each layer, the soil dry density and the cylinder volume used in the permeability test were considered. This experiment was conducted after 48 h of placing the test samples were placed in the apparatus cell (saturation period) to achieve optimal test conditions, including water-saturated soil voids free of air bubbles and steady-state flow with no variations in the hydraulic gradient. The results of these tests are summarized in Table 4.

Table 4. Summary of permeability (k) for sandy soil after a saturation period of 48 hours

Soil Type	Lime + Fly ash (% by weight)	The permeability (m/min)
Shell soil (sand with gravel)	0	$2.388 *10^{-2}$
Core soil (sand)	0	$4.902 *10^{-3}$
	3% Lime + 9% Fly ash	$2.977 *10^{-4}$
	5% Lime + 15% Fly ash	$7.140 *10^{-5}$
	7% Lime + 21% Fly ash	$4.626 *10^{-5}$
	9% Lime + 27% Fly ash	$1.875 *10^{-5}$

2.5. Numerical Model

The numerical analyses were performed using SLIDE 6.0 software, a two-dimensional limit equilibrium slope stability software, widely applied in previous studies to evaluate the factor of safety or probability of failure for both circular and non-circular failure surfaces in soil and rock slopes. The program assesses the stability of potential slip surfaces using vertical-slice limit equilibrium methods. In addition to slope stability calculations, SLIDE features a built-in finite element seepage analysis, which enables simulation of seepage behavior through earth dams under various hydraulic conditions [35, 36]. The numerical model incorporates the same geometry, material properties, and boundary conditions as the physical model to ensure comparability. SLIDE 6.0 uses the governing equation in the partial differential form of Darcy's law, which is applied to predict the phreatic line within the earth dam and to estimate seepage flow rates. Governing equations for seepage flow were solved using finite element analysis. The finite element mesh used in this analysis is shown in Figure 4. Three-node triangular elements were employed to discretize the domains, resulting in a total of 2285 elements. A query line was positioned 5 cm above the base of the dam, and sensor locations along this line were set to correspond to those of the experimental model.

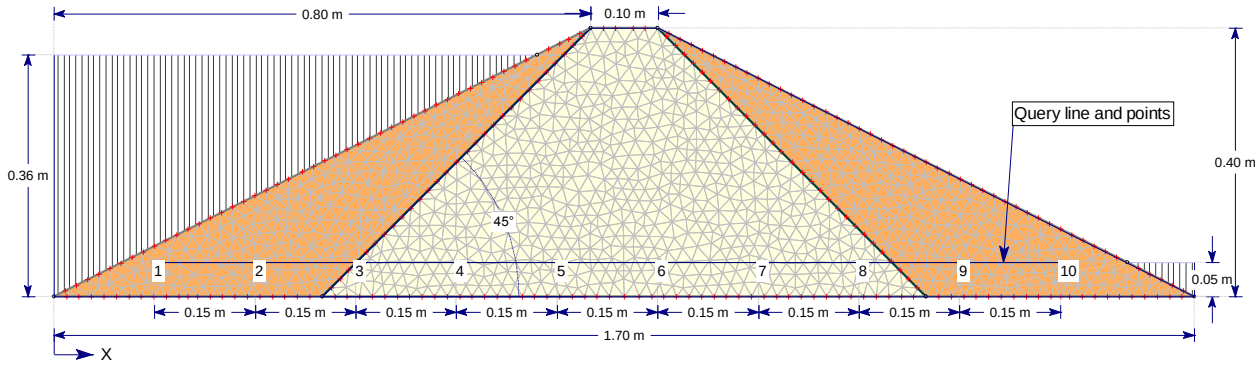

Figure 4. Cross-section of numerical earth dam model

3. Results and Discussion

3.1. Experimental Results

The physical model of the earthen dam constructed without lime and fly ash additives represents a zoned earth dam and served as the control. Each model's water storage was filled with a specific discharge of 2.496×10^{-3} m³/min; consequently, the upstream water level in each model increased gradually from zero to 36 centimeters after 15 min, when water was allowed to enter the basin from the water tank.

Figure 5 shows the pressure head readings over time obtained from ten sensors positioned 5 cm above the dam base for the control model and the treated models M-1 to M-4. Initially, all sensors in all models show zero pressure head values, indicating unsaturated conditions within the dam body. Sensors 1 through 3 exhibit a rapid increase in pressure head during the first few minutes, reaching values above 30 cm, which suggests their proximity to the upstream face, where water infiltration occurs early and saturation is achieved quickly. These readings also indicate that these zones possess higher permeability. In contrast, sensors 4 through 10 display delayed responses and lower pressure head values, implying their locations are farther from the upstream face or situated in less permeable regions. Then, sensor readings begin to stabilize, indicating the development of a steady-seepage condition.

Initial signs of seepage were observed on the downstream face of the control model after 46 minutes. The sensor response times, defined as the approximate time at which each sensor begins to rise significantly above zero (i.e., starts detecting pressure head increase), demonstrated a progressive delay as the seepage line advanced through the dam body. This delay became more pronounced in treated models, indicating that the presence of additives (lime and fly ash) significantly increased the time required for pore water pressure to be detected. For example, in model M-4 (Figure 5-E), Sensor 10 responded only after 1525 minutes, compared to just 46 minutes in the control model (Figure 5-A), reflecting a substantial improvement in seepage retardation due to the treatment.

In the control model (Figure 5-A), steady-state conditions were achieved after approximately 65 minutes. In contrast, the time required to reach steady-state in models M-1through M-4 (Figures 5-B to 5-E) was recorded as 160, 350, 700, and 1570 minutes, respectively, defined as the point at which both the seepage rate and the phreatic line became steady. These findings indicate a delay of approximately 1505 minutes in the M-4 model compared to the control.

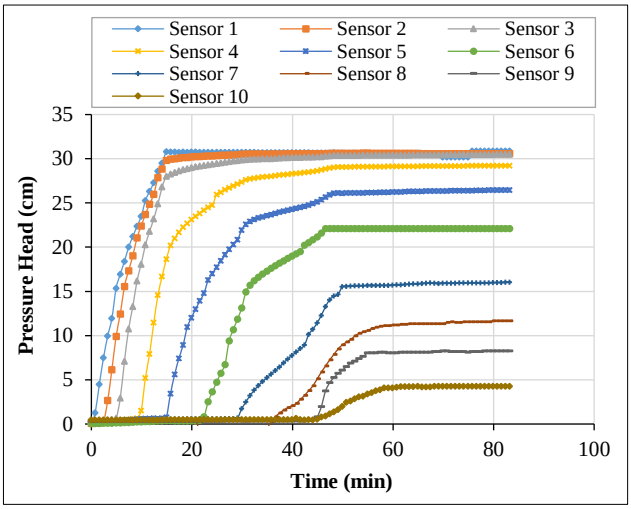

A: The control model

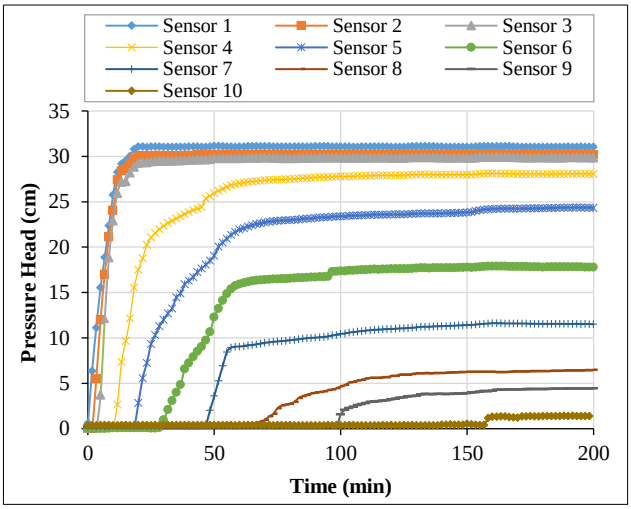

B: The M-1 model

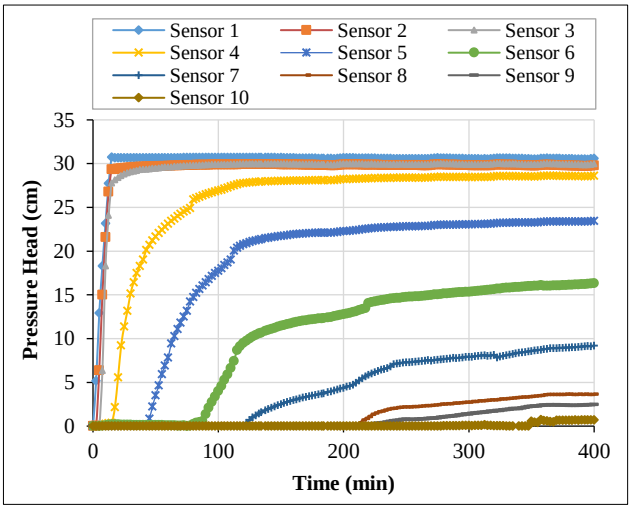

C: The M-2 model

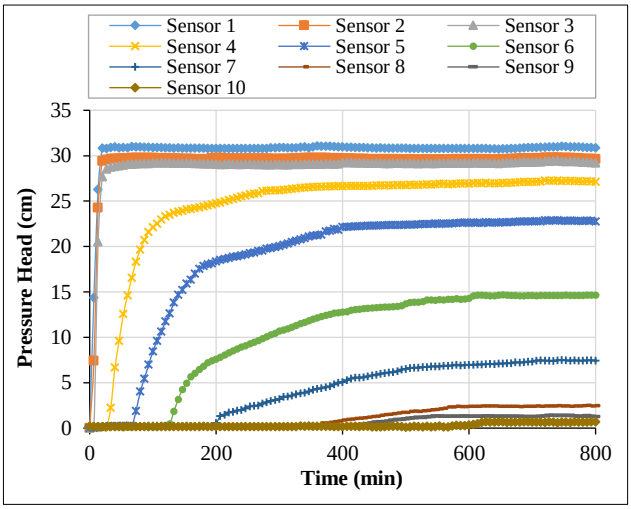

D: The M-3 model

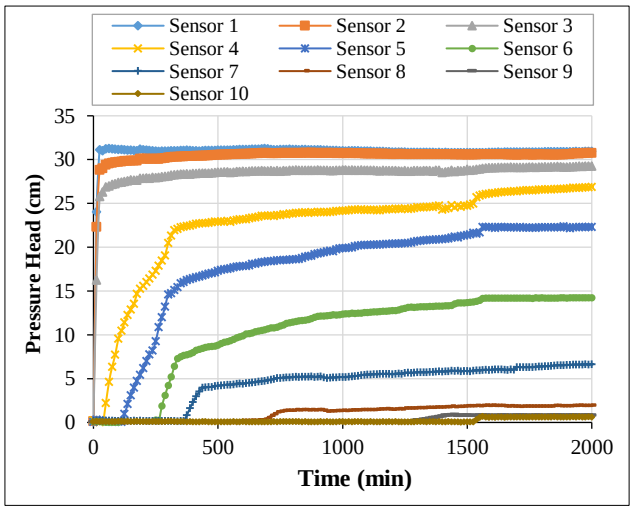

E: The M-4 model

Figure 5. The sensors' readings for pressure head along the control and treated models

Results of the steady-state phreatic line are presented in Figure 6, where it can be observed that the control model, represented by the uppermost curve, exhibits the highest pressure heads along the profile, indicating greater seepage flow and higher phreatic levels. In contrast, the treated models, particularly M-3 and M-4, show a significant downward shift in the phreatic line, indicating a reduction in pore water pressure and seepage potential due to improved soil

stabilization, resulting from the addition of lime and fly ash, which reduces soil permeability. The M-4 model shows the lowest phreatic line, lying well within the downstream face and close to the dam base, indicating the most effective seepage control.

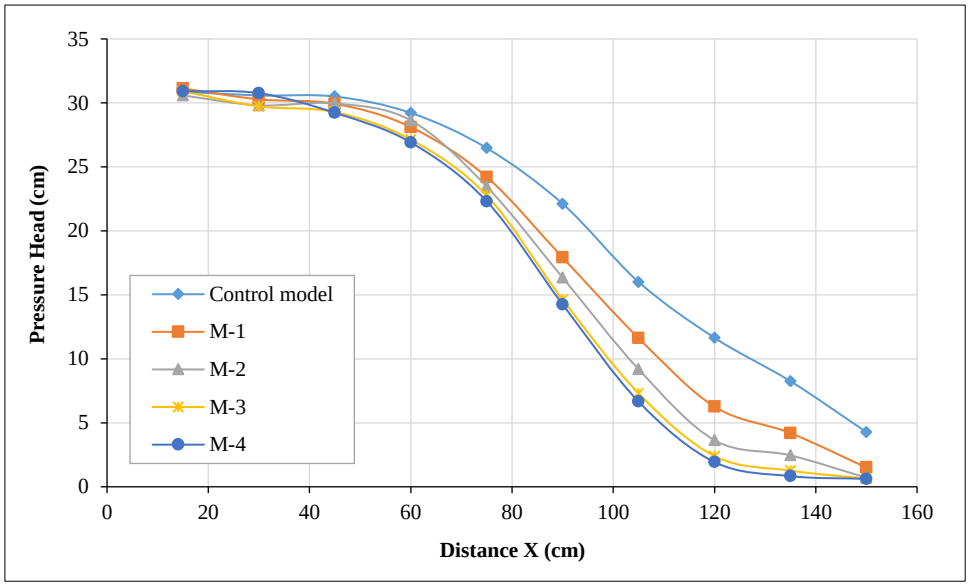

Figure 6. Steady-state phreatic line for the control model and models M-1 through M-4

The steady-state seepage rate for the control model was measured at 6.666×10^{-4} m³/min. Seepage reduction was achieved by enhancing the dam core with sandy soil stabilized with different proportions of lime and fly ash. The measured steady-state seepage rates for the treated models M-1 to M-4 were 1.888×10^{-4}, 8.555×10^{-5}, 2.45×10^{-5}, and 1.19×10^{-5} m³/min, respectively, corresponding to reductions of 71.6%, 87.1%, 96.3%, and 98.2%, respectively, compared to the control model.

3.2. Numerical Results

The steady-state seepage rates from the numerical simulations exhibit very close agreement with the experimental values across all models, with only minor differences observed (Figure 7). Furthermore, in Figure 8, steady-state phreatic lines are compared for some of the experimental and numerical models (control and M-4 models); the numerical results closely match the experimental results, with determination coefficients (R^2) exceeding 0.98. This level of agreement demonstrates that the numerical model developed using SLIDE 6.0 software can accurately simulate steady-state seepage conditions and phreatic surface positions. The computed contours in Figure 9 illustrate the steady-state pressure head distribution for the control model.

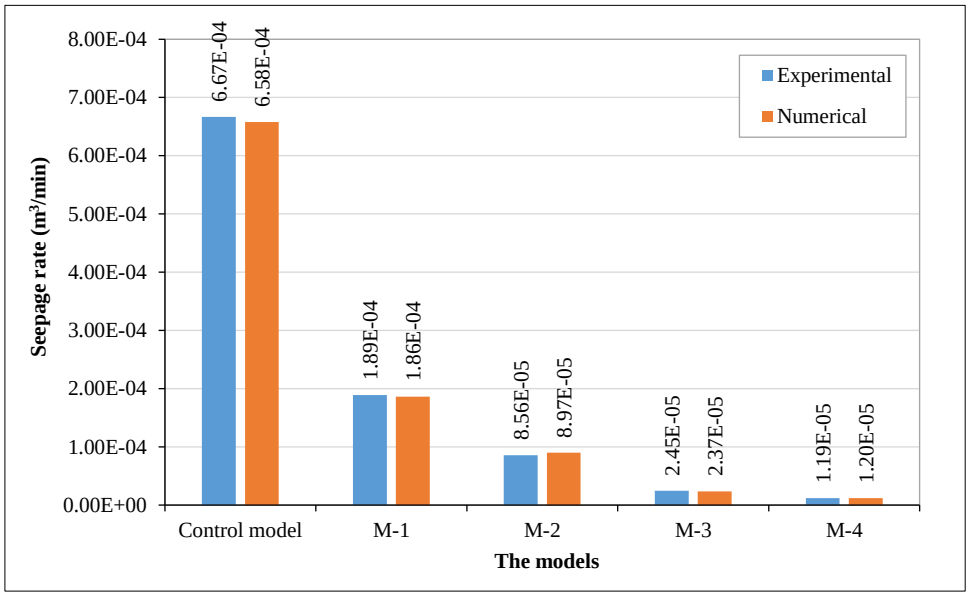

Figure 7. Steady-state seepage rate comparison for control and treated models (experimental vs. numerical)

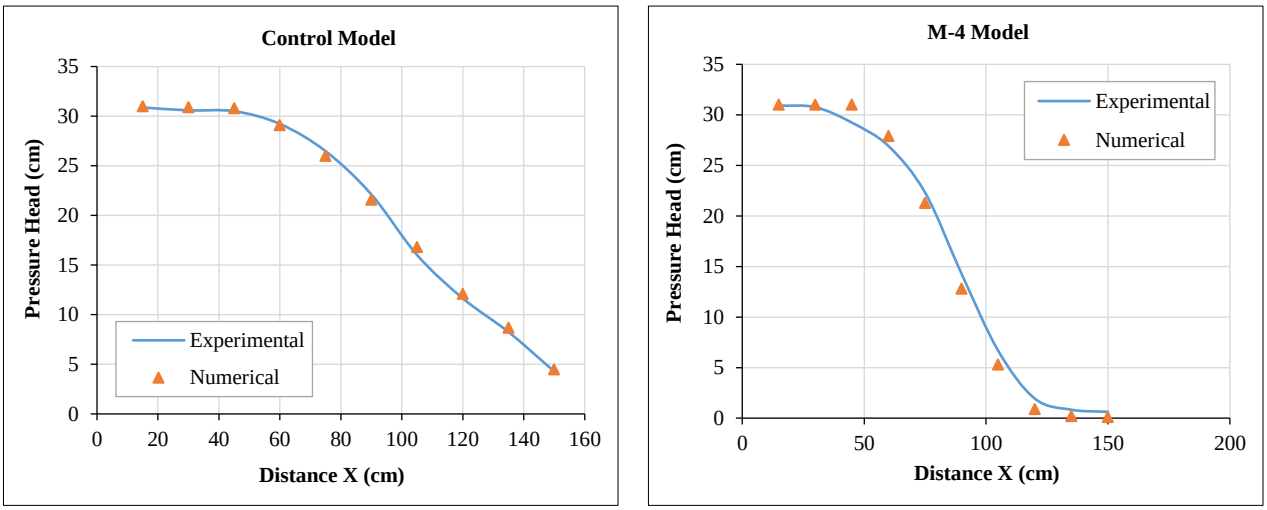

Figure 8. Comparison of steady-state phreatic lines between numerical and experimental results for the control and M-4 models

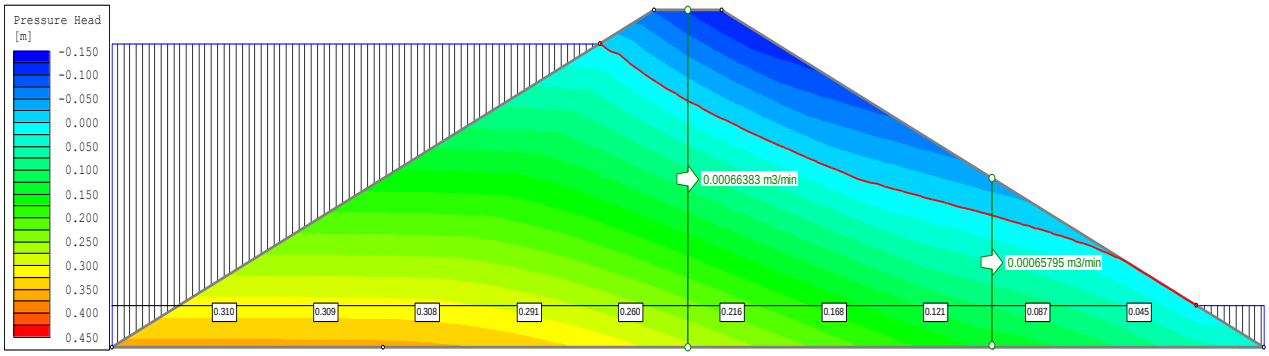

Figure 9. Computed contours of pressure head distribution in the control model

After validating the numerical model, the impact of core slope on seepage was examined. While the experimental models in this study used a core slope of 1:1 (H: V) for both treated and untreated cases, numerical simulations were extended to investigate alternative core slopes of 0.25:1, 0.5:1, and 0.75:1. Varying the slope changes the volume and shape of the core, which in turn influences seepage rates and pressure head. By assessing these configurations under steady-state conditions, the study aims to determine whether reducing the core slope, and thus the volume of impermeable material, can achieve comparable hydraulic performance while lowering construction costs.

Each of the four core slopes (1:1, 0.75:1, 0.5:1, and 0.25:1) was evaluated for all five models (Control, M-1, M-2, M-3, and M-4). Figure 10 presents the phreatic lines for the control and treated models (M-1 to M-4) under the effect of these different core slopes, measured along the query line. In line with the study objective of finding an optimal slope that balances hydraulic performance and material savings, the results indicate that a slope of 0.75:1 performs very close to the baseline 1:1 in all models, with only minor variations in phreatic line elevation.

The steeper core slopes (0.5:1 and 0.25:1) produce a noticeable upstream shift of the phreatic line and a clear rise in its elevation within the midsection of the core, along with a lowered phreatic line at the downstream end of the core zone, with the effect becoming more pronounced as the level of treatment increases. This is particularly evident in the highly treated models (M-3 and M-4), where the very low permeability of the core means that reducing its width significantly shortens the seepage path and concentrates flow through a narrower zone, resulting in greater changes to the phreatic line. In comparison, the control and lower-treatment models (M-1 and M-2) show smaller variations with the slope change, as their higher permeability allows seepage to redistribute more easily through the core, making the geometry less influential. From a design perspective, a 0.75:1 slope appears to offer a good compromise—retaining hydraulic performance similar to 1:1 while allowing for moderate core volume and cost reductions.

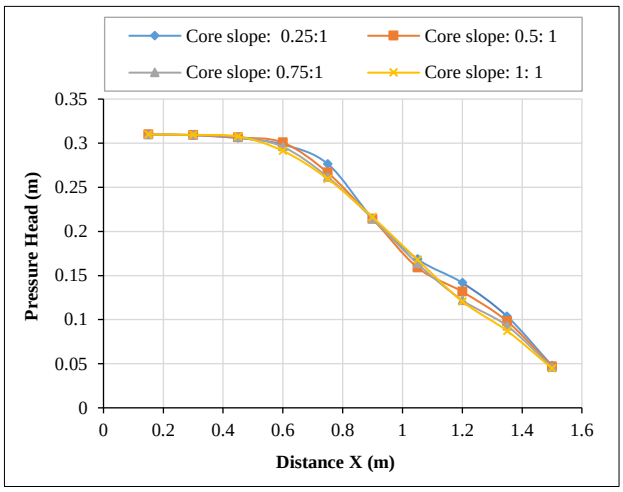

A: The control model

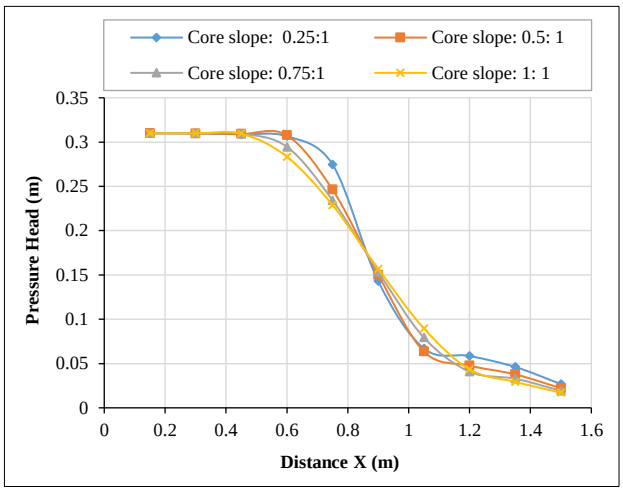

B: The M-1 model

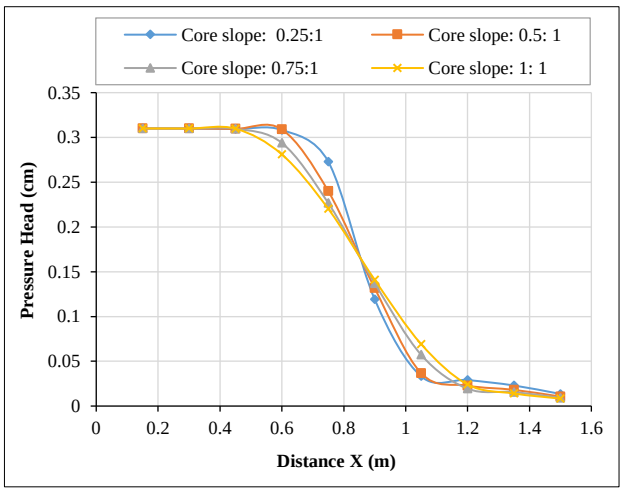

C: The M-2 model

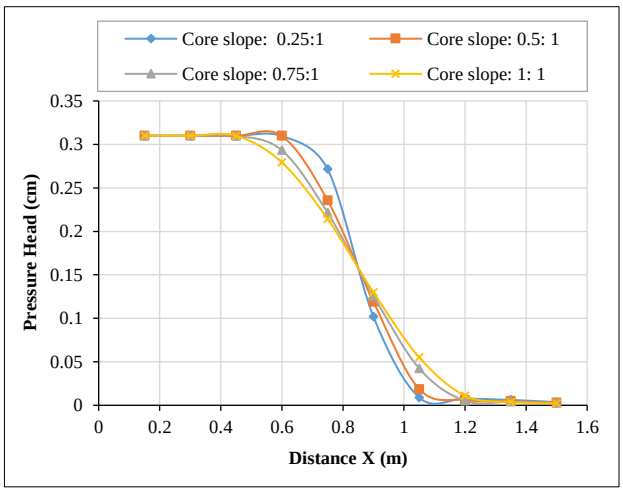

D: The M-3 model

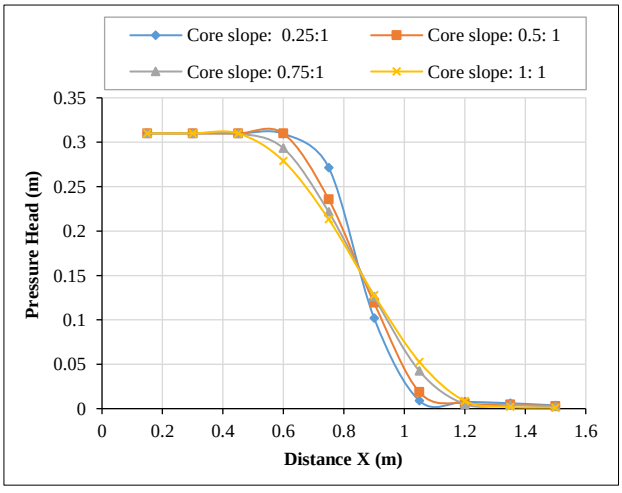

E: The M-4 model

Figure 10. Comparison of phreatic lines of the control and treated models for different core slopes

Table 5 shows the effect of core slope on steady-state seepage rates for the control and treated models. The results confirm that reducing the core slope generally increases seepage rates due to the reduced width of the low-permeability core zone along the seepage path. This shorter seepage path leads to increased hydraulic gradients, which in turn result in higher discharge. The increase is most pronounced at 0.25:1, with the control model showing a 32.1% rise and treated models reaching over 50% increases compared to 1:1. However, the slope of 0.75:1 produces only slight increases in seepage (around 10–12% across all models), which supports its selection as a preferred design option.

Table 5. Effect of core slope on steady-state seepage rate for the control and treated models in the numerical simulation

Model Code	Core Slope (H:V)	Seepage Rate (m^3/min)	Percentage increase in seepage (%)
Control model	1:01	6.57×10^{-4}	-
	0.75:1	7.33×10^{-4}	11.5
	0.5:1	8.10×10^{-4}	23.2
	0.25:1	8.68×10^{-4}	32.1
M-1 model	1:01	1.86×10^{-4}	-
	0.75:1	2.09×10^{-4}	12.3
	0.5:1	2.40×10^{-4}	29
	0.25:1	2.82×10^{-4}	51.6
M-2 model	1:01	8.97×10^{-5}	-
	0.75:1	9.95×10^{-5}	10.9
	0.5:1	1.15×10^{-4}	28.2
	0.25:1	1.38×10^{-4}	53.8
M-3 model	1:01	2.36×10^{-5}	-
	0.75:1	2.60×10^{-5}	10.1
	0.5:1	3.02×10^{-5}	28
	0.25:1	3.71×10^{-5}	57.2
M-4 model	1:01	1.20×10^{-5}	-
	0.75:1	1.32×10^{-5}	9.7
	0.5:1	1.53×10^{-5}	27.1
	0.25:1	1.89×10^{-5}	57.1

4. Conclusion

This study experimentally and numerically investigated the effectiveness of lime–fly ash mixtures in reducing seepage through zoned earth dams constructed with sandy cores. Based on the Laboratory tests, it can be concluded that treating the sandy core with lime–fly ash significantly reduces its permeability, leading to lower phreatic surfaces that lie well within the downstream face and closer to the dam base. Experimental results showed substantial delays in reaching steady-state conditions, with the treated models extending from 160 minutes in M-1 to 1570 minutes in M-4, compared to only 65 minutes in the control. Moreover, the treated models (M-1 to M-4) exhibited a pronounced decrease in steady-state seepage rates, achieving reductions of 71.6%, 87.1%, 96.3%, and 98.2%, respectively, compared to the control model. Numerical simulations, validated against experimental data ($R^2 > 0.98$), confirmed the reliability of the modelling approach in predicting seepage rates and phreatic-line distributions. The parametric analysis indicated that reducing the core slope from the baseline 1:1 to steeper geometries (1:0.75, 1:0.5, and 1:0.25) generally increased the steady-state seepage rates. However, results also showed that a core slope of 0.75:1 provided hydraulic performance comparable to the baseline 1:1 slope, with only minor increases in seepage, thereby offering a more economical design option through reduced core volume.

The findings highlight that lime–fly ash treatment can transform locally available sandy soils into impervious core materials, providing an environmentally sustainable and economically efficient alternative where natural clay is limited. This study investigated seepage behavior through the dam, while the mechanical properties, such as stability, were not examined. Future research should focus on verifying these properties. If lime and fly ash additives are found to enhance the strength of the dam, they may be recommended for use in dam construction.

5. Declarations

5.1. Author Contributions

Conceptualization, A.M.M. and A.A.A.; methodology, A.M.M. and S.I.K.; software, A.M.M.; validation, A.M.M., A.A.A., and S.I.K.; formal analysis, A.M.M.; investigation, A.M.M., A.A.A., and S.I.K.; resources, A.M.M.; data curation, A.M.M.; writing—original draft preparation, A.M.M.; writing—review and editing, A.A.A. and S.I.K.; visualization, A.M.M.; supervision, A.A.A. and S.I.K.; project administration, A.M.M.; funding acquisition, A.M.M. All authors have read and agreed to the published version of the manuscript.

5.2. Data Availability Statement

The data presented in this study are available on request from the corresponding author.

5.3. Funding

The authors received no financial support for the research, authorship, and/or publication of this article.

5.4. Conflicts of Interest

The authors declare no conflict of interest.

6. References

[1] Chen, S., Zhong, Q., & Shen, G. (2019). Numerical modeling of earthen dam breach due to piping failure. Water Science and Engineering, 12(3), 169–178. doi:10.1016/j.wse.2019.08.001.

[2] Houghtalen, R. J., Akan, A. O., & Hwang, N. H. (2017). Fundamentals of hydraulic engineering systems. Pearson Education, London, United Kingdom.

[3] Budhu, M. (2000). Soil Mechanics and Foundations (2nd Ed.). John Wiley & Sons, New York, United States.

[4] Hussein, S. S., Majeed, Z. H., & Obead, I. H. (2025). Microstructural Attributes for Soft Soils Affected by Salts during Soaking and Seepage. Civil Engineering Journal, 11(5), 1772–1785. doi:10.28991/CEJ-2025-011-05-04.

[5] Bashir, A., Chaudhry, R., Qureshi, A. L., Memon, U., & Bheel, N. (2022). Understanding the Seepage Behavior of Nai Gaj Dam through Numerical Analysis. Engineering, Technology & Applied Science Research, 12(1), 8085–8089. doi:10.48084/etasr.4560.

[6] Kanchana, H. J., & Prasanna, H. S. (2015). Adequacy of Seepage Analysis in Core Section of the Earthen Dam with Different Mix Proportions. Aquatic Procedia, 4, 868–875. doi:10.1016/j.aqpro.2015.02.109.

[7] Chun, B. S., Lee, Y. J., & Chung, H. I. (2006). Effectiveness of leakage control after application of permeation grouting to earth fill dam. KSCE Journal of Civil Engineering, 10(6), 405–414. doi:10.1007/bf02823979.

[8] Devipriya, V. P., Chandrakaran, S., & Rangaswamy, K. (2022). Seepage behavior of soil mixed with randomly distributed recycled plastic materials. Water Science and Engineering, 15(3), 257–264. doi:10.1016/j.wse.2022.06.002.

[9] Taghvaei, P., Mousavi, S. F., Shahnazari, A., Karami, H., & Shoshpash, I. (2019). Experimental and Numerical Modeling of Nano-clay Effect on Seepage Rate in Earth Dams. International Journal of Geosynthetics and Ground Engineering, 5(1), 1. doi:10.1007/s40891-018-0152-8.

[10] Alzamily, Z. N., & Sh. Abed, B. (2022). Experimental and theoretical investigations of seepage reduction through zoned earth dam material with special core. Materials Today: Proceedings, 61, 998–1005. doi:10.1016/j.matpr.2021.10.283.

[11] Haman, D. Z., Smajstrla, A. G., Zazueta, F. S., & Clark, G. A. (1990). Selecting a method for sealing ponds in Florida. Institute of Food and Agricultural Sciences, University of Florida, Florida, United States.

[12] Shuhaib, Z. K., & Khassaf, S. I. (2023). Experimental and numerical evaluation of tire rubber powder effectiveness for reducing seepage rate in earth dams. Open Engineering, 13(1), 1–13. doi:10.1515/eng-2022-0422.

[13] Onyelowe, K. C., Nimbalkar, A., Reddy, N. G., Baldovino, J. de J. A., Hanandeh, S., & Ebid, A. M. (2023). Seepage Analysis and Optimization of Reservoir Earthen Embankment with Double Textured HDPE Geo-Membrane Barrier. Civil Engineering Journal (Iran), 9(11), 2736–2751. doi:10.28991/CEJ-2023-09-11-07.

[14] Das, B. M. (2011). Principles of Foundation Engineering (7th Ed.). Cengage Learning, Stamford, United States.

[15] Fang, H. Y. (1991). Foundation Engineering Handbook (2nd Ed.). Chapman & Hall, Boca Raton, United States.

[16] Arora, K. R. (1992). Soil Mechanics and Foundation Engineering in S.I. Units, 3rd Ed. Standard Publishers Distributors, New Delhi, India.

[17] Murthy, V. N. S. (2007). Advanced foundation engineering. Chennai: CBS publishers & distributors, New Delhi, India.

[18] Indiramma, P., Sudharani, C., & Needhidasan, S. (2020). Utilization of fly ash and lime to stabilize the expansive soil and to sustain pollution free environment - An experimental study. Materials Today: Proceedings, 22, 694–700. doi:10.1016/j.matpr.2019.09.147.

[19] Arslan, E., Develioglu, I., & Pulat, H. F. (2025). A Comparative Study on the Performance of Freeze-Thaw Cycled Alluvial Soils Stabilized with Lime and Fly Ash. Karadeniz Fen Bilimleri Dergisi, 15(3), 1094–1118. doi:10.31466/kfbd.1609555.

[20] Sambre, T., Endait, M., & Patil, S. (2024). Sustainable soil stabilization of expansive soil subgrades through lime-fly ash admixture. Discover Civil Engineering, 1(1), 65. doi:10.1007/s44290-024-00063-1.

[21] Arias-Jaramillo, Y. P., Gómez-Cano, D., Carvajal, G. I., Hidalgo, C. A., & Muñoz, F. (2023). Evaluation of the Effect of Binary Fly Ash-Lime Mixture on the Bearing Capacity of Natural Soils: A Comparison with Two Conventional Stabilizers Lime and Portland Cement. Materials, 16(11), 13996. doi:10.3390/ma16113996.

[22] Di Sante, M., Khan, M. K., Calò, L., Fratalocchi, E., & Mazzieri, F. (2025). The Combined Use of Fly Ash and Lime to Stabilize a Clayey Soil: A Sustainable and Promising Approach. Geosciences (Switzerland), 15(9), 346. doi:10.3390/geosciences15090346.

[23] Sharif, S., Ali, K., Khan, M. A., & Sajid, M. (2025). Cost implication of utilizing fly ash and lime for stabilizing clayey soil as subgrade for construction of pavement. Discover Civil Engineering, 2(1), 1–20. doi:10.1007/s44290-025-00329-2.

[24] Bhoi, K. D., Desai, P. P., Kambale, A. A., Patil, M. R., & Savyanavar, R. V. (2024). Soil stabilization by using lime and fly ash. International Journal of Research in Engineering, Science and Management, 7(4), 79-81.

[25] Swamynaidu, M., & Tyagi, A. (2024). Hydraulic conductivity of cement and fly ash stabilised clay mixes – Application to soil mixing techniques for seepage barrier construction. Construction and Building Materials, 431, 136533. doi:10.1016/j.conbuildmat.2024.136533.

[26] Husein, F., & Chemeda, Y. C. (2018). Lime stabilization of highly plastic clayey soil for the impervious core of embankment dam: The case of Gidabo dam, Ethiopia. Ethiopian Journal of Science and Sustainable Development, 5(2), 27–39.

[27] Garzón, E., Cano, M., ÒKelly, B. C., & Sánchez-Soto, P. J. (2016). Effect of lime on stabilization of phyllite clays. Applied Clay Science, 123, 329–334. doi:10.1016/j.clay.2016.01.042.

[28] Islam, M. S., Islam, T., & Khatun, N. (2021). Permeability Alteration of Low Plastic Clay and Poorly Graded Sand Using Lime and Fly Ash. Indian Geotechnical Journal, 51(5), 967–978. doi:10.1007/s40098-020-00493-5.

[29] United States. Bureau of Reclamation. (1987). Design of small dams. Bureau of Reclamation, US Department of the Interior, Washington, United States.

[30] Garg, S. K. (2006). Irrigation Engineering and Hydraulic Structures. Khanna Publishers, New Delhi, India.

[31] Iraqi Specification No. 807. (2004). Lime Used in Buildings. Ministry of Planning, Baghdad, Iraq.

[32] ASTM C618-22. (2023). Standard Specification for Coal Fly Ash and Raw or Calcined Natural Pozzolan for Use in Concrete. ASTM International, Pennsylvania, United States. doi:10.1520/C0618-22.

[33] ASTM D2434-68(2006). (2019). Standard Test Method for Permeability of Granular Soils (Constant Head). ASTM International, Pennsylvania, United States. doi:10.1520/D2434-68R06.

[34] ASTM D5084-16. (2016). Standard Test Methods for Measurement of Hydraulic Conductivity of Saturated Porous Materials Using a Flexible Wall Permeameter. ASTM International, Pennsylvania, United States. doi:10.1520/D5084-16.

[35] Aziz, Y. W., Ibrahim, A. H., & Mohammedamin, O. K. (2023). Effect of Core Geometry on Earth Dam Slope Stability. Tikrit Journal of Engineering Sciences, 30(2), 41–45. doi:10.25130/tjes.30.2.5.

[36] Khanna, R., Datta, M., & Ramana, G. V. (2017). Influence of core thickness on stability of downstream slope of earth and rockfill dams under end-of-construction and steady-state-seepage: A comparison. International Journal of Geotechnical Engineering, 13(1), 25–31. doi:10.1080/19386362.2017.1318230.